

MEASUREMENT OF THE LONGITUDINAL PROTON STRUCTURE FUNCTION AT THE H1 EXPERIMENT*

IVANA PICURIC on behalf of the H1 Collaborations

University of Montenegro, Faculty of Natural Sciences and Mathematics, P. O. BOX 211, 81001
Podgorica, Montenegro, E-mail: ivana@rc.pmf.ac.me

Received September 12, 2012

Abstract. This report presents the most recent measurement of the longitudinal structure function F_L obtained from e^+p interactions recorded by the H1 experiment at HERA accelerator. The data at different proton beam energies of 460 GeV, 575 GeV and 920 GeV are used to determine F_L . The measurements are obtained for low values of photon virtuality Q^2 down to 1.5 GeV² and low values of Bjorken variable x down to $2.7 \cdot 10^{-5}$. Direct measurement of F_L allows also to measure structure function F_2 which represents a model independent determination without extra assumption on F_L . The data are compared with the predictions based on NLO and NNLO QCD calculations.

Key words: deep inelastic scattering, proton structure function.

1. INTRODUCTION

Deep inelastic lepton-nucleon scattering (DIS) plays a pivotal role in determining the structure of the proton. The electron-proton collider HERA covers a wide range of absolute four-momentum transfer squared, Q^2 , and of Bjorken x . Previous measurements of the DIS cross section, performed by the H1 and ZEUS collaborations, using data at proton beam energies of $E_p = 820$ GeV and $E_p = 920$ GeV and a lepton beam energy of $E_e = 27.6$ GeV, as well as their combination, have enabled studies of perturbative Quantum Chromodynamics (QCD) with unprecedented precision. These measurements are complemented here with new data including the data taken at $E_p = 460$ GeV and $E_p = 575$ GeV [1].

At low Q^2 , the scattering cross section is defined by the two structure functions, F_2 and F_L . In a reduced form, the double differential cross section is given by:

$$\sigma_r(x, Q^2) = \frac{Q^4}{2\pi\alpha^2 [1 + (1 - y^2)]} \frac{d^2\sigma}{dx dQ} = F_2(x, Q^2) - \frac{y^2}{1 + (1 - y^2)} F_L(x, Q^2). \quad (1)$$

* Paper presented at the 8th General Conference of Balkan Physical Union, July 5–7, 2012, Constanța, Romania.

Here α is the fine structure constant and $0 \leq y \leq 1$ is the process inelasticity which is related to Q^2 , x and the centre-of-mass energy squared $s = 4E_e E_p$ by $y = Q^2 / sx$. The two structure functions are defined by the cross sections for the scattering of the longitudinally and transversely polarised photons off protons σ_L and σ_T as

$$F_L(x, Q^2) = \frac{Q^2}{4\pi^2\alpha} (1-x)\sigma_L, \quad (2)$$

$$F_2(x, Q^2) = \frac{Q^2}{4\pi^2\alpha} (1-x)(\sigma_L + \sigma_T). \quad (3)$$

These relations are valid to good approximation at low x and imply that $0 \leq F_L \leq F_2$. To disentangle the two structure functions in a model-independent way, measurements at different values of s are required.

Using the ratio $R(x, Q^2)$, defined as:

$$R = \frac{\sigma_L}{\sigma_T} = \frac{F_L}{F_2 - F_L}, \quad (4)$$

the reduced cross section in equation 1 can also be written as:

$$\sigma_r = F_2(x, Q^2) \left[1 - f(y) \frac{R}{1+R} \right], \quad (5)$$

where

$$f(y) = y^2 / (1 + (1 - y^2)). \quad (6)$$

The measurements are used to test several phenomenological and QCD models describing the low x behaviour of the DIS cross section. The phenomenological models include the power law dependence of F_2 and several dipole models applicable at low $x < 0.01$. For the first time, dipole model analyses are extended to account for the non-negligible valence quark contributions at small x . Fits using the DGLAP evolution equations at NLO are applied for $Q^2 \geq 3.5 \text{ GeV}^2$. For the DGLAP fits, different treatments of the heavy quark contributions are compared. A study of possible non-DGLAP contributions at low x and low Q^2 is performed by varying kinematic cuts applied to the data. The dipole and DGLAP models are compared to with other by performing fits in a common kinematic domain.

2. DETERMINATION OF THE STRUCTURE FUNCTION F_L

The structure function F_L is determined using the separate $E_p = 460 \text{ GeV}$ and $E_p = 575 \text{ GeV}$ samples and the published 920 GeV data from [2, 3]. To determine F_L , common values of the (x, Q^2) grid centres are required for all centre-of-mass

energies. The published 920 GeV data have therefore been reanalysed using the binning adopted for the F_L analysis. To determine F_L , the data measured at high y for $E_p = 460$ GeV are combined with the data at intermediate y for $E_p = 575$ GeV and low y for $E_p = 920$ GeV. The usage of the published 920 GeV data compared to a new analysis of the HERA-II data is motivated by a wider Q^2 acceptance at low y , extending to $Q^2 = 1.5$ GeV². The determination of the structure function F_L depends on the treatment of the relative normalisations and systematic uncertainties of the data sets. A straightforward but simplified procedure was adopted in [10] where the data sets were normalised to each other at low y . The values of the structure function F_L were determined in straight-line fits to the reduced cross section as a function of $y^2/(1 + (1 - y)^2)$ in each (x, Q^2) bin using the statistical and uncorrelated systematic uncertainties. The correlated systematic errors were determined using an offset method. An illustration of this procedure, applied to the cross-section data from the current analysis, is shown in Fig. 1.

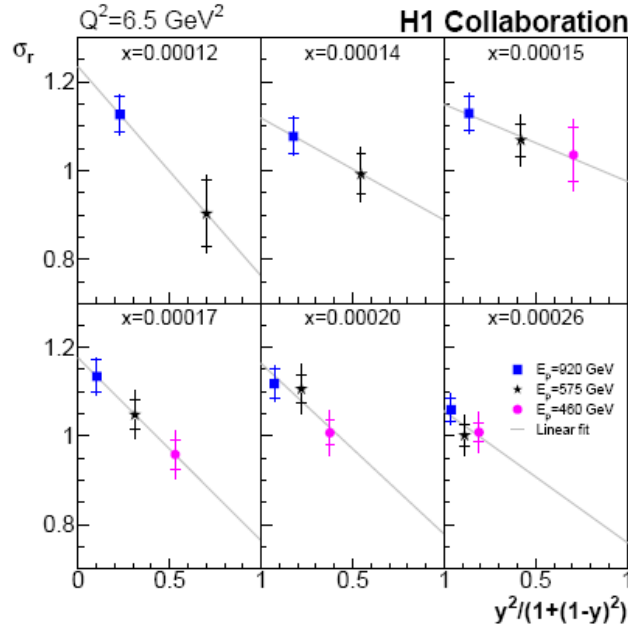


Fig. 1 – The reduced DIS cross section σ_r as a function of $y^2/(1 + (1 - y)^2)$ for six values of x at $Q^2 = 6.5$ GeV², measured for proton beam energies of $E_p = 920, 575$ and 460 GeV. The inner error bars denote the statistical error, the outer error bars show statistical and systematic uncertainties added in quadrature. The luminosity uncertainty is not included in the error bars. The slope of the straight-line fits is determined by the structure function $F_L(x, Q^2)$.

The measured structure function $F_L(x, Q^2)$ is shown in Fig. 2. Measurements with total uncertainties below 0.3 for $Q^2 \leq 35$ GeV² and below 0.4 for $Q^2 = 45$ GeV² are presented.

The measurement spans over two decades in x at low x , from $x = 0.00002$ to $x = 0.002$. The data are compared to the result of the DGLAP ACOT fit, which is described in section 3.2. The structure function F_2 measured for the corresponding bins is shown together with F_L in Fig. 3. Note that compared to the previous determinations of F_2 by the H1 collaboration, this measurement represents a model independent determination without extra assumptions on F_L .

3. PHENOMENOLOGICAL ANALYSIS

The combined cross-section data for $E_p = 460, 575$ and $E_p = 820, 920$ GeV are used for several phenomenological analyses. The fits are applied to the combined reduced cross-section measurements accounting for correlations between the data points. In the following, the quality of different fits is compared in terms of χ^2 / n_{dof} . Since the systematic uncertainties dominate over statistics, and they are estimated conservatively, in several cases χ^2 / n_{dof} is observed to be less than unity. This, however, does not prevent the comparison of quality among different fits with the same number of degrees of freedom in terms of $\Delta\chi^2$ since the average error overestimation, approximated as χ^2 / n_{dof} , does not exceed 5–10%.

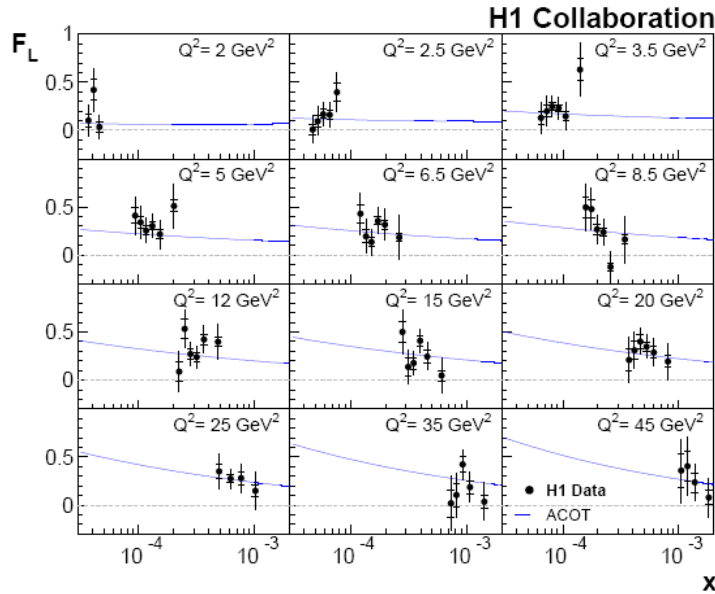


Fig. 2 – The proton structure function $F_L(x, Q^2)$. The inner error bars represent statistical error, the full error bars include the statistical and systematic uncertainties added in quadrature, excluding 0.5% global normalisation uncertainty. The curves represent predictions of the DGLAP fit in the ACOT scheme.

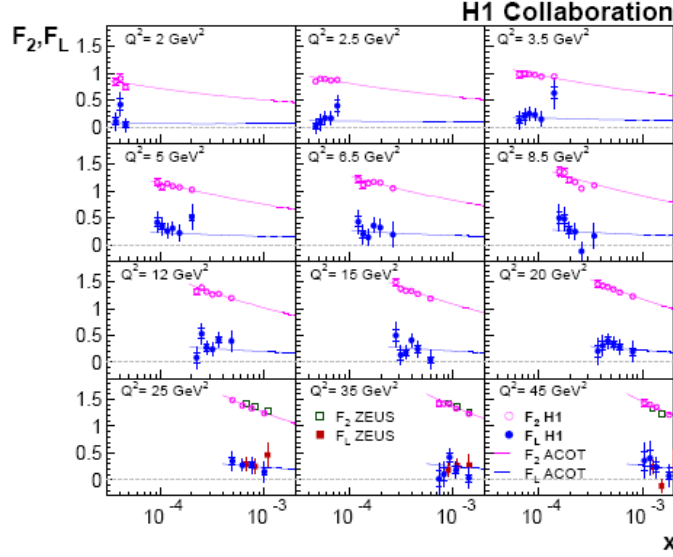


Fig. 3 – The proton structure functions $F_2(x, Q^2)$ and $F_L(x, Q^2)$. The inner error bars represent statistical error, the full error bars include the statistical and systematic uncertainties added in quadrature, excluding 0.5% global normalisation uncertainty. The curves represent predictions of the DGLAP fit in the ACOT scheme for the structure functions F_2 and F_L . The measurements from ZEUS are also shown.

3.1. λ FIT

The increase of the structure function F_2 for $x \rightarrow 0$ can be approximated by a power law in x , $F_2 = c(Q^2)x^{-\lambda(Q^2)}$. This simple parameterisation was shown to describe previous H1 data rather well for $x < 0.01$ [4]. In the recent H1 analysis [2], a fit was performed to the measured reduced cross section, σ_r , represented as

$$\sigma_r(Q^2, x) = c(Q^2)x^{-\lambda(Q^2)} \left[1 - \frac{y^2}{1 + (1 - y^2)} \frac{R}{1 + R} \right]. \quad (7)$$

The combined H1 data are fitted using the offset method to evaluate systematic uncertainties. The parameters obtained in the fits as a function of Q^2 are shown in Fig. 4. The parameter λ exhibits an approximately linear increase as a function of $\ln Q^2$ for $Q^2 \geq 2 \text{ GeV}^2$. For lower Q^2 , the variation of λ deviates from that linear dependence. The normalisation coefficient $c(Q^2)$ rises with increasing Q^2 for $Q^2 < 2 \text{ GeV}^2$ and is consistent with a constant behaviour for higher Q^2 , as in [4]. The total χ^2 of the fit is $\chi^2/n_{\text{dof}} = 538/350$, when the uncertainties are taken as the statistical and uncorrelated systematic uncertainties added in quadrature. Values of χ^2/n_{dof} significantly larger than unity may arise in the offset method because it does not take into account the correlated systematic uncertainties. Studies show that the largest contribution to the χ^2 arises from the $1 < Q^2 < 10 \text{ GeV}^2$ domain.

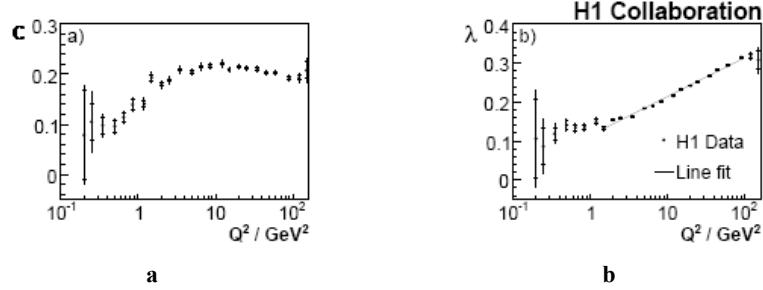


Fig. 4 – Coefficients c and λ , as defined in equation 7, determined from a fit to the data as a function of Q^2 . The inner error bars represent statistical uncertainties. The outer error bars contain the statistical and systematic uncertainties added in quadrature. The line in b) is from a straight-line fit for $Q^2 \geq 2 \text{ GeV}^2$.

3.2. DGLAP FIT

The new combined H1 data are used together with the previously published high $Q^2 \geq 90 \text{ GeV}^2$ H1 data [5–7] as input to a DGLAP pQCD fit analysis to NLO,

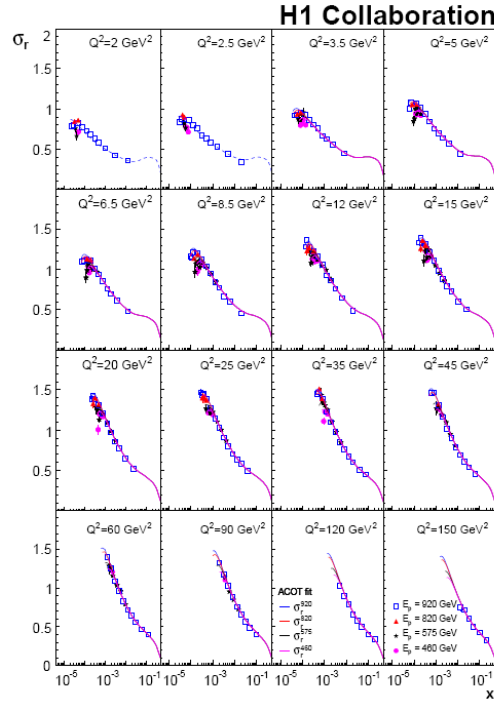


Fig. 5 – The reduced cross-section measurements taken at different proton beam energies E_p compared to the DGLAP fit in the ACOT scheme (shown by curves) for $2.0 \leq Q^2 \leq 150 \text{ GeV}^2$. The dashed line for $Q^2 \leq 2.5 \text{ GeV}^2$ corresponds to the fit extrapolation.

with the main objective of studying F_L predictions. The initial fits are performed using the same parameterisation type as for the HERAPDF1.0 fit [8], which has only one free polynomial parameter, Eu_v . For this parameterisation, the ACOT and RT heavy flavour schemes are compared. Both fits give good descriptions of the data, but the ACOT fit, which has $\chi^2/n_{\text{dof}} = 722.7/782$, is superior to the RT fit, with $\chi^2/n_{\text{dof}} = 773.2/782$, by about 50 units. Therefore, the ACOT fit is chosen for further more detailed investigations. The best fit is obtained with the extra free parameters Du_v and Eu_v resulting in a $\chi^2/n_{\text{dof}} = 715.2/781$. Figure 5 compares the fit result to the low Q^2 H1 data. As a consistency check, a fit using the RT heavy flavour scheme is repeated. A similar increase in χ^2 of about 50 units is observed in this case. The sensitivity of the fit to the inclusion of low Q^2 data is studied by varying the Q_{min}^2 cut. The fit obtained with Q_{min}^2 cut of 7.5 GeV^2 falls significantly below the data at small x when extrapolating to the low Q^2 region. Figure 6 shows gluon and sea-quark distributions for different values of Q_{min}^2 at the evolution starting scale $Q_0^2 = 1.9 \text{ GeV}^2$. A change of Q_{min}^2 from 1.5 GeV^2 to 7.5 GeV^2 leads to an increase of the gluon distribution while the sea-quark distribution becomes smaller at low x .

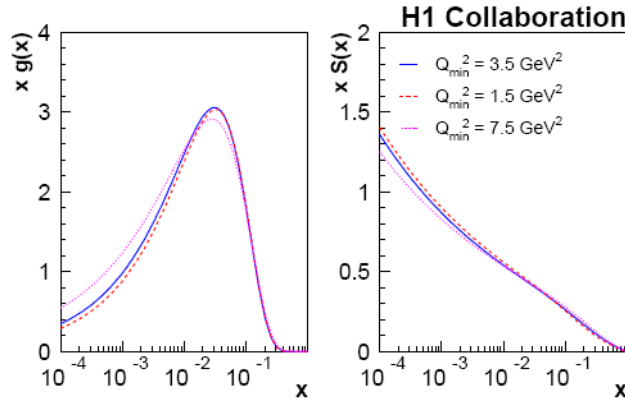


Fig. 6 – Gluon and sea quark PDFs shown at the starting scale $Q_0^2 = 1.9 \text{ GeV}^2$ for different values of Q_{min}^2 .

4. CONCLUSIONS

The data at $E_p = 460 \text{ GeV}$ and $E_p = 575 \text{ GeV}$, together with the measurements at $E_p = 920 \text{ GeV}$ are used to determine the structure function F_L . This extraction applies a novel method which takes into account the correlations of data points due to systematic uncertainties. This is the first measurement at low $1.5 \leq Q^2 \leq 45 \text{ GeV}^2$ and $2.7 \times 10^{-5} < x < 2 \times 10^{-3}$, which became possible by employing a dedicated backward silicon tracker for the electron reconstruction.

The data are reasonably well reproduced by the predictions based on NLO and NNLO QCD. The combined H1 data are subjected to phenomenological analyses. The rise of the structure function F_2 towards low x is examined using power-law fits. As in previous H1 analyses, the power-law exponent λ is found to be approximately constant for $Q^2 \leq 2 \text{ GeV}^2$ but increases linearly with $\ln Q^2$ for higher Q^2 values. The data are found to be well described by an NLO DGLAP QCD analysis. The ACOT and the RT schemes are used, which differ in the treatment of the heavy-flavour and higher-order F_L contributions to the cross section. A comparison of ACOT and RT based fits to the data reveals a significant preference for the ACOT treatment.

Acknowledgments. I thank all colleagues who were involved in obtaining the results presented here.

REFERENCES

1. F. Aaron et al. [H1 Collaboration], Eur. Phys. J., **C 71**, 1579 (2011).
2. F. Aaron *et al.* [H1 Collaboration], Eur. Phys. J., **C 64**, 561 (2009).
3. F. Aaron *et al.* [H1 Collaboration], Eur. Phys. J., **C 63**, 625 (2009).
4. C. Adloff *et al.* [H1 Collaboration], Phys. Lett., **B 520**, 183 (2001).
5. C. Adloff *et al.* [H1 Collaboration], Eur. Phys. J., **C 13**, 609 (2000).
6. C. Adloff *et al.* [H1 Collaboration], Eur. Phys. J., **C 19**, 269 (2001).
7. C. Adloff *et al.* [H1 Collaboration], Eur. Phys. J., **C 30**, 1 (2003).
8. F. Aaron *et al.* [H1 and ZEUS Collaborations], JHEP, **1001**, 109 (2010).
9. N. N. Nikolaev and B. G. Zakharov, Z. Phys., **C 49**, 607 (1991).
10. F. Aaron *et al.* [H1 Collaboration], Phys. Lett., **B 665**, 139 (2008).